Nonresonant hyper-Raman and hyper-Rayleigh scattering in benzene and pyridine

John P. Neddersen,[a] Sarah A. Mounter, James M. Bostick, and Carey K. Johnson[b]
Department of Chemistry, University of Kansas, Lawrence, Kansas 66045

(Received 20 October 1988; accepted 17 January 1989)

Nonresonant hyper-Raman and hyper-Rayleigh spectra excited at 1064 nm are reported for neat benzene and pyridine. The theory of Herzberg–Teller vibronic coupling in nonresonant and preresonant hyper-Raman scattering is developed. Nonresonant hyper-Raman scattering is shown to be vibronically induced by modes that efficiently couple strongly allowed one-photon and two-photon transitions. A weak and broad (55 cm^{-1}) hyper-Rayleigh band was observed in benzene and attributed to collective scattering, while in pyridine, a much more intense and much narrower hyper-Rayleigh band was observed. Only the a_{2u} vibration (ν_{11}) was observed in the hyper-Raman spectrum of benzene, while several strong bands were observed in pyridine. Possible vibronic-coupling pathways are discussed for these modes. In addition, the observed hyper-Raman spectrum of pyridine is compared to a recent calculation.

I. INTRODUCTION

Benzene and pyridine have often played the roles of prototypes in spectroscopic studies of aromatic and hetrocyclic molecules, and many studies have been undertaken on the vibrational and electronic properties of these molecules. In this paper we report the first hyper-Raman and hyper-Rayleigh spectra of these compounds. Our purpose was to generate unenhanced and nonresonant hyper-Raman and hyper-Rayleigh spectra of these molecules, and to explore the mechanism by which these spectra are induced. Of particular interest to us is the role of vibronic interaction in hyper-Raman scattering (hereafter HRS), and the participation of collective motions in hyper-Rayleigh scattering (HRlS).

It has been recognized for many years that a potentially rich source of information regarding intramolecular and intermolecular dynamics in liquids lies in the dependence of the hyperpolarizability on vibrational, rotational, and translational motions.[1–5] HRS and HRlS were first reported by Terhune *et al.* for water and fused quartz.[6] Since then, HRS spectra have been published for several liquids,[7–11] as well as solids and gases.[12,13] More recently, several workers have also reported *resonant* HRS,[14–16] and apparent surface enhancement of HRS has also been observed.[17–19] Nevertheless, the application of HRS and HRlS to the study of molecular vibrations and liquid-state dynamics has been limited in practice by very low HRS and HRlS cross sections, even at peak laser intensities of 10^9 W/cm^2. In this research we have exploited the properties of mode-locked, Q-switched CW Nd:YAG lasers to generate peak powers about 3 orders of magnitude larger at a moderately high repetition rate.

This paper is organized as follows: In Sec. II experimental methods are reported. A vibronic coupling theory of HRS is discussed in Sec. III, and results and discussion are presented in Sec. IV, The HRS spectra of benzene and pyridine are discussed in terms of the vibronic mechanism of HRS, and are related to a recent calculation[19] of the bulk pyridine HRS spectrum.

II. EXPERIMENTAL METHOD

Pyridine and benzene (Burdick and Jackson HPLC grade) samples were filtered through a micropore filter into a quartz sample cell. Infrared light (1064 nm) from a mode-locked, Q-switched Nd:YAG laser (Quantronix 116) was focused by a 25 mm focal-length lens into the sample cell. The laser produced pulse trains of 100 ps pulses at a repetition rate of 1 kHz. Peak powers were ~0.4 MW, and peak intensities were estimated to be $\sim 10^{12}$ W/cm^2.[20] Scattered light was collected at 90° with f/1.2 optics, and focused into a spectrometer (Instruments S.A. HR-640). For Raman spectra, 532 nm excitation was employed. The slit width was 500 μm for HRS and HRlS spectra, and 10 μm for Raman spectra. The polarization properties of the 1800 grove per mm holographic grating resulted in the detection almost exclusively of light polarized parallel to the excitation beam polarization. The dispersed light was detected by an intensified Reticon (Princeton Instruments IRY-1000) and analyzed. Typically, 9 to 25 integration periods of about 2 min each were summed to obtain the HRS and HRlS signals.

III. THEORY

Hyper-Raman and hyper-Rayleigh scattering are represented by six time-ordered diagrams. In the usual case where a single beam is incident on the sample, these reduce to three distinct time orderings. The corresponding time-ordered diagrams are shown in Fig. 1. The theory of HRS has been discussed by several workers[5,16,21,22] and selection rules determined.[23–25] In this section we discuss HRS in the Condon and Herzberg–Teller (HT) approximations. Our treatment is in this respect similar to previous treatments by Petrov,[26] and Chung and Ziegler.[16] We choose, however, to group first-order HT coupling terms according to the intermediate

[a] ACS-PRF Summer Research Fellow. Current address: Carroll College, Waukesha, WI 53186.
[b] Author to whom correspondence should be addressed.

 0021-9606/89/094719-08$02.10

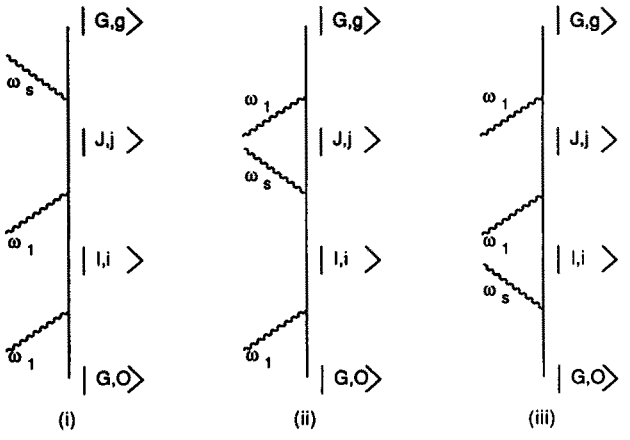

FIG. 1. Time-ordered diagrams for hyper-Raman ($2\omega_1 \neq \omega_s$) and hyper-Rayleigh ($2\omega_1 \cong \omega_s$) scattering. Diagram (i) represents the two-photon and one-photon resonant term; diagram (ii) the one-photon resonant term; diagram (iii) the term with no resonances.

state in which the vibronic coupling occurs, and include all three time orderings.

The hyperpolarizability tensor may be written down from the time-ordered diagrams in Fig. 1. One finds, in a molecule-fixed axis system with coordinates labeled by a, b, c,

$$\beta_{cba}(\omega_s;\omega_1,\omega_1) = \sum_{J,j}\sum_{I,i}\left[\frac{\langle G,g|\mu_c|J,j\rangle\langle J,j|\mu_b|I,i\rangle\langle I,i|\mu_a|G,0\rangle}{(\omega_{Ii,G0}-\omega_1)(\omega_{Jj,G0}-2\omega_1)} + \frac{\langle G,g|\mu_b|J,j\rangle\langle J,j|\mu_c|I,i\rangle\langle I,i|\mu_a|G,0\rangle}{(\omega_{Ii,G0}-\omega_1)(\omega_{Jj,G0}-\omega_1+\omega_s)} + \frac{\langle G,g|\mu_b|J,j\rangle\langle J,j|\mu_a|I,i\rangle\langle I,i|\mu_c|G,0\rangle}{(\omega_{Ii,G0}+\omega_s)(\omega_{Jj,G0}-\omega_1+\omega_s)}\right], \quad (1)$$

where G, I, and J label electronic states, g, i, and j are vibrational levels, and $\omega_{Aa,Bb} = \omega_A + \omega_a - \omega_B - \omega_b$, and $\omega_s = 2\omega_1 - \omega_g$.

In the Born–Oppenheimer approximation, the adiabatic wave functions are expanded in a crude adiabatic basis set as

$$|G(\mathbf{Q})\rangle = |G(\mathbf{0})\rangle + \sum_{\alpha}\sum_{G'\neq G}|G'(\mathbf{0})\rangle\frac{h^{\alpha}_{G'G}}{\epsilon^0_G-\epsilon^0_{G'}}Q_\alpha, \quad (2)$$

where

$$h^{\alpha}_{G'G} = \langle G'(\mathbf{0})|\left(\frac{\partial H_E}{\partial Q_\alpha}\right)_0|G(\mathbf{0})\rangle$$

with analogous expansions for $|I(\mathbf{Q})\rangle$ and $|J(\mathbf{Q})\rangle$, where H_E is the electronic Hamiltonian (excluding nuclear kinetic energy). Substituting Eq. (2) and analogous expressions for $|I\rangle$ and $|J\rangle$ into Eq. (1), and keeping only zero and first-order HT coupling terms, we find, in analogy with Tang and Albrecht's treatment of Raman scattering,[27]

$$\beta_{cba} = A + B + B' + C \quad (3)$$

where

$$A = \sum_{J,j}\sum_{I,i}\left[\frac{\mu^{(c)}_{GJ}\mu^{(b)}_{JI}\mu^{(a)}_{IG}}{(\omega_{Ii,G0}-\omega_1)(\omega_{Jj,G0}-2\omega_1)} + \frac{\mu^{(b)}_{GJ}\mu^{(c)}_{JI}\mu^{(a)}_{IG}}{(\omega_{Ii,G0}-\omega_1)(\omega_{Jj,G0}-\omega_1+\omega_s)} + \frac{\mu^{(b)}_{GJ}\mu^{(a)}_{JI}\mu^{(c)}_{IG}}{(\omega_{Ii,G0}+\omega_s)(\omega_{Jj,G0}-\omega_1+\omega_s)}\right]\langle g|j\rangle\langle j|i\rangle\langle i|0\rangle \quad (4)$$

$$B = \sum_{J,j}\sum_{I,i}\sum_{J'}\sum_{\alpha}\left\{\left[\frac{\mu^{(c)}_{GJ'}h^{\alpha}_{J'J}\mu^{(b)}_{JI}\mu^{(a)}_{IG}}{(\omega_{Ii,G0}-\omega_1)(\omega_{Jj,G0}-2\omega_1)} + \frac{\mu^{(b)}_{GJ'}h^{\alpha}_{J'J}\mu^{(c)}_{JI}\mu^{(a)}_{IG}}{(\omega_{Ii,G0}-\omega_1)(\omega_{Jj,G0}-\omega_1+\omega_s)} + \frac{\mu^{(b)}_{GJ'}h^{\alpha}_{J'J}\mu^{(a)}_{JI}\mu^{(c)}_{IG}}{(\omega_{Ii,G0}+\omega_s)(\omega_{Jj,G0}-\omega_1+\omega_s)}\right]\times\frac{\langle g|Q_\alpha|j\rangle\langle j|i\rangle\langle i|0\rangle}{\epsilon^0_J-\epsilon^0_{J'}} + \left[\frac{\mu^{(c)}_{GJ}h^{\alpha}_{JJ'}\mu^{(b)}_{J'I}\mu^{(a)}_{IG}}{(\omega_{Ii,G0}-\omega_1)(\omega_{Jj,G0}-2\omega_1)} + \frac{\mu^{(b)}_{GJ}h^{\alpha}_{JJ'}\mu^{(c)}_{J'I}\mu^{(a)}_{IG}}{(\omega_{Ii,G0}-\omega_1)(\omega_{Jj,G0}-\omega_1+\omega_s)} + \frac{\mu^{(b)}_{GJ}h^{\alpha}_{JJ'}\mu^{(a)}_{J'I}\mu^{(c)}_{IG}}{(\omega_{Ii,G0}+\omega_s)(\omega_{Jj,G0}-\omega_1+\omega_s)}\right]\times\frac{\langle g|j\rangle\langle j|Q_\alpha|i\rangle\langle i|0\rangle}{\epsilon^0_J-\epsilon^0_{J'}}\right\} \quad (5)$$

$$B' = \sum_{J,j}\sum_{I,i}\sum_{I'}\sum_{\alpha}\left\{\left[\frac{\mu^{(c)}_{GJ}\mu^{(b)}_{JI'}h^{\alpha}_{I'I}\mu^{(a)}_{IG}}{(\omega_{Ii,G0}-\omega_1)(\omega_{Jj,G0}-2\omega_1)} + \frac{\mu^{(b)}_{GJ}\mu^{(c)}_{JI'}h^{\alpha}_{I'I}\mu^{(a)}_{IG}}{(\omega_{Ii,G0}-\omega_1)(\omega_{Jj,G0}-\omega_1+\omega_s)} + \frac{\mu^{(b)}_{GJ}\mu^{(a)}_{JI'}h^{\alpha}_{I'I}\mu^{(c)}_{IG}}{(\omega_{Ii,G0}+\omega_1)(\omega_{Jj,G0}-\omega_1+\omega_s)}\right]\times\frac{\langle g|j\rangle\langle j|Q_\alpha|i\rangle\langle i|0\rangle}{\epsilon^0_I-\epsilon^0_{I'}} + \left[\frac{\mu^{(c)}_{GJ}\mu^{(b)}_{JI}h^{\alpha}_{II'}\mu^{(a)}_{I'G}}{(\omega_{Ii,G0}-\omega_1)(\omega_{Jj,G0}-2\omega_1)} + \frac{\mu^{(b)}_{GJ}\mu^{(c)}_{JI}h^{\alpha}_{II'}\mu^{(a)}_{I'G}}{(\omega_{Ii,G0}-\omega_1)(\omega_{Jj,G0}-\omega_1+\omega_s)} + \frac{\mu^{(b)}_{GJ}\mu^{(a)}_{JI}h^{\alpha}_{II'}\mu^{(c)}_{I'G}}{(\omega_{Ii,G0}+\omega_s)(\omega_{Jj,G0}-\omega_1+\omega_s)}\right]\times\frac{\langle g|j\rangle\langle j|i\rangle\langle i|Q_\alpha|0\rangle}{\epsilon^0_I-\epsilon^0_{I'}}\right\} \quad (6)$$

$$C=\sum_{J,j}\sum_{I,i}\sum_{G'}\sum_{\alpha}\Bigg\{\Bigg[\frac{\mu_{GJ}^{(c)}\mu_{JI}^{(b)}\mu_{IG'}^{(a)}h_{G'G}^{\alpha}}{(\omega_{Ii,G0}-\omega_1)(\omega_{Jj,G0}-2\omega_1)}$$
$$+\frac{\mu_{GJ}^{(b)}\mu_{JI}^{(c)}\mu_{IG'}^{(a)}h_{G'G}^{\alpha}}{(\omega_{Ii,G0}-\omega_1)(\omega_{Jj,G0}-\omega_1+\omega_s}$$
$$+\frac{\mu_{GJ}^{(b)}\mu_{JI}^{(a)}\mu_{IG'}^{(c)}h_{G'G}^{\alpha}}{(\omega_{Ii,G0}+\omega_s)(\omega_{Jj,G0}-\omega_1+\omega_s)}\Bigg]$$
$$\times\frac{\langle g|j\rangle\langle j|i\rangle\langle i|Q_\alpha|0\rangle}{\epsilon_G^0-\epsilon_{G'}^0}$$
$$+\Bigg[\frac{h_{GG'}^{\alpha}\mu_{G'J}^{(c)}\mu_{JI}^{(b)}\mu_{IG}^{(a)}}{(\omega_{Ii,G0}-\omega_1)(\omega_{Jj,G0}-2\omega_1)}$$
$$+\frac{h_{GG'}^{\alpha}\mu_{G'J}^{(b)}\mu_{JI}^{(c)}\mu_{IG}^{(a)}}{(\omega_{Ii,G0}-\omega_1)(\omega_{Jj,G0}-\omega_1+\omega_s)}$$
$$+\frac{h_{GG'}^{\alpha}\mu_{G'J}^{(b)}\mu_{JI}^{(a)}\mu_{IG}^{(c)}}{(\omega_{Ii,G0}+\omega_s)(\omega_{Jj,G0}-\omega_1+\omega_s)}\Bigg]$$
$$\times\frac{\langle g|Q_\alpha|j\rangle\langle j|i\rangle\langle i|0\rangle}{\epsilon_G^0-\epsilon_{G'}^0}\Bigg\}, \tag{7}$$

where $\mu_{GJ}^{(a)}=\langle G|(\mathbf{0}|\mu_a|J(\mathbf{0})\rangle$, etc.

The A term is the Condon approximation for Eq. (1), and the terms B, B', and C carry first-order HT coupling in state J, I, and G, respectively. Since we wish to consider nonresonant HRS, we retain all three terms of Eq. (1) in our expressions for A, B, B', and C. Thus Eqs. (4)–(7) contain expressions for diagrams (ii) and (iii) in Fig. 1, in addition to the resonant terms given by Petrov.[26] Our terms B, B', and C are combined in a single expression [but only for diagram (i)] by Chung and Ziegler[16] (their B term) and we omit second-order vibronic effects (their C term).

For nonresonant HRS, in the large electronic energy gap approximation,[28] one can write

$$\omega_{Ii,G0}\cong\omega_{I,G}$$
$$\omega_{Jj,G0}\cong\omega_{J,G} \tag{8}$$

and carry out the sum over vibrational levels i and j. For the A term, the product of vibrational overlap integrals reduces to $\langle g|0\rangle=\delta_{g,0}$. Thus, the nonresonant A term contributes only to HRlS, and not to HRS, just as, in nonresonant Raman scattering, the A term contributes only to Rayleigh scattering in the large electronic energy gap limit. That is, *nonresonant HRS is vibronically induced*. We note in addition that the A term is inoperative for centrosymmetic molecules in HRlS, and in resonant as well as nonresonant HRS. The terms B, B', and C contribute to nonresonant and resonant HRS. We note in particular that the vibrations allowed by the B and B' terms are those which vibronically couple two-photon allowed and one-photon allowed states.

We turn now to consider HRS intensities in the preresonance regime. By preresonance is meant the regime where the detuning from resonance (two-photon or one-photon) is large relative to vibrational frequencies, but where the large electron energy gap approximation is insufficiently accurate. We employ the method of Yeung *et al.*[29] for treating preresonance Raman intensities, and define, for the first term in Eq. (4),

$$S_{I,J}=\sum_{i,j}\frac{\langle g|j\rangle\langle j|i\rangle\langle i|0\rangle}{(\Delta_I+\Delta_i)(\Delta_J+\Delta_j)} \tag{9}$$

where the detuning of ω_1 and $2\omega_1$ from state $|I,i\rangle$ and $|J,j\rangle$, respectively, is given by

$$\omega_{Ii,G0}-\omega_1=\Delta_I+\Delta_i, \tag{10}$$

$$\omega_{Jj,G0}-2\omega_1=\Delta_J+\Delta_j. \tag{11}$$

Here Δ_I and Δ_J are the detuning of ω_1 and $2\omega_1$, respectively, from the vertical electronic energy gap at the ground-state equilibrium coordinates, and

$$\Delta_i=\omega_i(I)-\omega_0(G)-\delta_{\rm ad}(I), \tag{12}$$

where $\omega_i(I)$ and $\omega_0(G)$ are the vibrational energies in levels i and 0 of state I and G, respectively, and $\delta_{\rm ad}(I)$ is the difference between the adiabatic and vertical electronic energy gaps in state I. $S_{I,J}$ can be expanded as

$$S_{I,J}=\frac{1}{\Delta_I\Delta_J}\sum_{n=0}\sum_{m=0}\sum_{i,j}S_{I,J}^{n,m}, \tag{13}$$

where

$$S_{I,J}^{n,m}=\frac{(-1)^n(-1)^m}{\Delta_I^n\Delta_J^m}\langle g|j\rangle\langle j|i\rangle\langle i|0\rangle\Delta_i^n\Delta_j^m. \tag{14}$$

We assume that

$$\left|\frac{\Delta_i}{\Delta_I}\right|<1;\quad\left|\frac{\Delta_j}{\Delta_J}\right|<1. \tag{15}$$

The sum over vibrational levels can now be evaluated.[29] Carrying out the sums over j and i, we find, for the A term:

$$A_1=\sum_J\sum_I\sum_\alpha\Bigg[\frac{\mu_{GJ}^{(c)}\mu_{JI}^{(b)}\mu_{IG}^{(a)}}{\Delta_I\Delta_J}\left(-\frac{h_{JJ}^{\alpha}}{\Delta_J}-\frac{h_{II}^{\alpha}}{\Delta_I}+\cdots\right)$$
$$+\frac{\mu_{GJ}^{(b)}\mu_{JI}^{(c)}\mu_{IG}^{(a)}}{\Delta_I\Delta_J'}\left(-\frac{h_{JJ}^{\alpha}}{\Delta_J'}-\frac{h_{II}^{\alpha}}{\Delta_I}+\cdots\right)$$
$$+\frac{\mu_{GJ}^{(b)}\mu_{JI}^{(a)}\mu_{IG}^{(c)}}{\Delta_I'\Delta_J'}\left(-\frac{h_{JJ}^{\alpha}}{\Delta_J'}-\frac{h_{II}^{\alpha}}{\Delta_I'}+\cdots\right)\Bigg]\langle g|Q_\alpha|0\rangle. \tag{16}$$

Here

$$\Delta_J'=\omega_{J,G}+\delta_{\rm ad}(J)-\omega_1+\omega_s \tag{17}$$

and

$$\Delta_I'=\omega_{I,G}+\delta_{\rm ad}(I)+\omega_s \tag{18}$$

are always positive. Since h_{II}^{α} and h_{JJ}^{α} are nonvanishing only for totally symmetric vibrations, the lowest-order enhancement of A as resonance is approached is by totally symmetric vibrations (in noncentrosymmetric molecules).

The vibronic contributions to preresonance HRS can be evaluated in a similar manner. In what follows we neglect frequency changes (quadratic electron–vibration coupling terms) upon electronic excitation. These effects can easily be incorporated, as described by Yeung *et al.*[29] We present here the results for the preresonace expansion of the B and B' terms. For the terms in B corresponding to the first time-ordered diagram in Fig. 1:

$$B_1 = \sum_J \sum_I \sum_{J'} \sum_\alpha \left[\frac{\mu^{(c)}_{GJ'} h^{\alpha}_{J'J} \mu^{(b)}_{JI} \mu^{(a)}_{IG}}{\Delta_I \Delta_J (\epsilon^\circ_J - \epsilon^\circ_{J'})} (1 + \cdots) + \frac{\mu^{(c)}_{GJ} h^{\alpha}_{JJ'} \mu^{(b)}_{J'I} \mu^{(a)}_{IG}}{\Delta_I \Delta_J (\epsilon^\circ_J - \epsilon^\circ_{J'})} \times (1 - \frac{\omega_\alpha}{\Delta_J} + \cdots) \right] \langle g|Q_\alpha|0\rangle . \quad (19)$$

For the terms in B corresponding to the second time-ordered diagram (Fig. 1), the coordinate labels for the transition dipole are permuted, and Δ_J is replaced with Δ'_J in Eq. (19). For the third time ordering, Δ_J and Δ_I are replaced with Δ'_J and Δ'_I. (The primed denominators are, of course, always nonresonant.)

Similarly, we find for the B' term, Eq. (6),

$$B'_1 = \sum_J \sum_I \sum_{I'} \sum_\alpha \left[\frac{\mu^{(c)}_{GJ} \mu^{(b)}_{JI'} h^{\alpha}_{I'I} \mu^{(a)}_{IG}}{\Delta_I \Delta_J (\epsilon^\circ_I - \epsilon^\circ_{I'})} \left(1 - \frac{\omega_\alpha}{\Delta_J} + \cdots\right) + \frac{\mu^{(c)}_{GJ} \mu^{(b)}_{JI} h^{\alpha}_{II'} \mu^{(a)}_{I'G}}{\Delta_I \Delta_J (\epsilon^\circ_I - \epsilon^\circ_{I'})} \times \left(1 - \frac{\omega_\alpha}{\Delta_J} - \frac{\omega_\alpha}{\Delta_I} + \cdots\right) \right] \langle g|Q_\alpha|0\rangle . \quad (20)$$

The expressions for the second and third time orderings can be written by adapting Eq. (20) in the same way as described above for Eq. (19).

We note that the leading terms in A carry a different frequency dependence than the leading terms in B and B' as the preresonance regime is approached, just as in preresonance Raman, the Condon and vibronic contributions differ in their preresonance excitation profiles.[29] In the preresonance regime for $2\omega_1$, where Δ_J is small but Δ_I is still large, the leading terms in B and B' carry the frequency dependence $\Delta_I^{-1}\Delta_J^{-1}$ while the leading term in A carries the frequency dependence $\Delta_I^{-1}\Delta_J^{-2}$. Thus the preresonance excitation profiles of the Condon and vibronic contributions in HRS will differ as the two-photon resonance is approached.

IV. RESULTS AND DISCUSSION

A. Benzene

1. Hyper-Rayleigh scattering

The HRIS and HRS spectra of benzene are shown in Figs. 2 and 3. Since benzene is centrosymmetric, HRIS is allowed only by cooperative scattering due to correlations in position and orientation of neighboring molecules.[3,30] An integrated HRIS signal and depolarization ratio were measured for benzene by Kielich and co-workers[31] (with an interference filter), but the HRIS spectrum has not been reported previously. The HRIS spectrum in Fig. 2 has a linewidth (FWHM) of 55 cm^{-1}, implying extremely fast (subpicosecond) decay of the correlation responsible for cooperative elastic scattering. The band is Lorentzian within experimental accuracy. Interestingly, cooperative scattering in the HRIS spectrum of CCl_4 contributes a broad band with FWHM $\sim$ 55 cm^{-1} to its HRIS line.[5] Broad cooperatively scattered bands were also observed in C_2Cl_4.[32]

2. Hyper-Raman scattering

The HRS spectum of benzene can contain no Condon-allowed contribution (in the dipole approximation), since

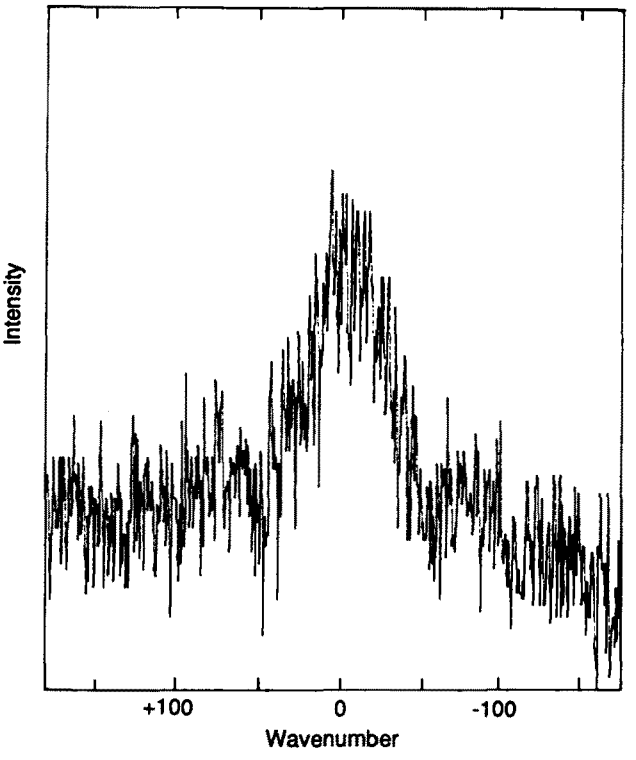

FIG. 2. Hyper-Rayleigh spectrum of benzene excited at 1064 nm. The peak signal is 80 counts per channel (1 channel = 0.50 cm^{-1}). This signal is the sum of 25 Reticon exposures of 132 s per exposure.

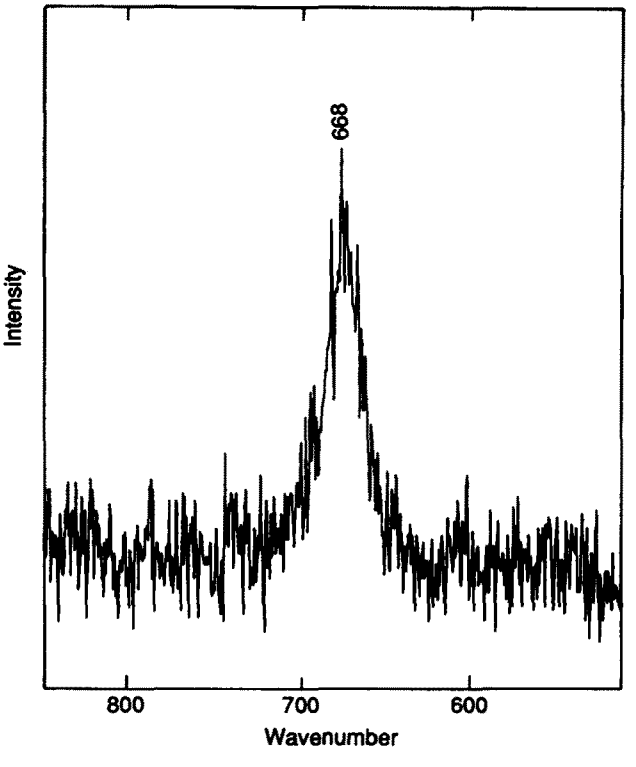

FIG. 3. Hyper-Raman scattering in benzene excited at 1064 nm. The peak signal is 200 counts per channel, collected in a total of nine Reticon exposures of 132 s per exposure.

the A term vanishes, even under resonance or preresonance conditions. (We expect cooperative effects in HRS to be negligible.) Thus the HRS spectrum of benzene probes vibronic coupling via vibrations with u parity. For benzene, the hyper-Raman allowed fundamentals are the a_{2u}, b_{1u}, b_{2u}, e_{1u}, and e_{2u} modes.[23,24] However, despite extensive scans of the regions from 400 to 3000 cm^{-1}, we observed only the a_{2u} vibration ν_{11} at 668 cm^{-1} (Fig. 3). Based on the signal-to-noise ratio of our scans, the intensity of any other mode must be at least 5× less than that of ν_{11}.

Since HRS in benzene is vibronically induced, the intensity of scattering into a particular allowed vibrational mode is determined by the efficiency of that mode in coupling electronic states, and by the nature of the electronic states involved. We assume that, as in resonance Raman scattering,[27] the C term is less important than the B and B' terms. A vibration can appear via the B and B' terms [Eqs. (4) and (5)] by vibronic coupling of two-photon allowed states (A_{1g}, E_{1g}, or E_{2g}) with a strongly one-photon allowed state (A_{2u} or E_{1u}).

The most plausible explanation for the intensity of ν_{11} (the only a_{2u} vibration of benzene) relative to any other HRS-allowed mode is a strong contribution from HT coupling of an E_{1g} and an E_{1u} state by the a_{2u} mode. This coupling mechanism allows intensity borrowing from the strongly allowed ($f\sim 1$) 185 nm E_{1u} state. Furthermore, a strong two-photon transition to an E_{1g} Rydberg 3s state has been identified at 180–200 nm in pure liquid benzene,[33] very near the E_{1u} state. Mode ν_{11} is an out-of-plane vibration where the carbon atoms move together with equal displacements in the same direction.[34] Since the nodal patterns perpendicular to the plane of the molecule are the same in the E_{1g} and E_{1u} states, qualitative considerations suggest efficient coupling by ν_{11}. The near match in energy of the E_{1g} and E_{1u} states leads to enhancement of the B and B' terms for these states. A vibronic coupling mechanism involving these electronic states was also suggested by Gerrity *et al.* to explain their observation of the first overtone of ν_{11} in the 204–213 nm resonance Raman spectra of benzene vapor.[35] Participation of a two-photon allowed E_{2g} state is unlikely, because it would be coupled by an a_{2u} vibration with dipole-forbidden E_{2u} states. We cannot, however, exclude HT coupling of A_{1g} with A_{2u} states. An A_{2u} state (3p Rydberg state or $\sigma\pi^*$) with vibronic activity in ν_{11} has been observed by two-photon resonant multiphoton ionization.[36] However, an A_{1g} excited state has not been identified. Vibronic coupling of E_{1g} and E_{1u} can occur both in the virtual state J (B term) or in the virtual state I (B' term).

The lack of comparable intensity of other vibrations in the HRS spectrum of benzene is evidence that other HT coupling pathways (e.g., coupling of E_{1g} and E_{1u} staes by e_{2u} vibrations $\nu_{16a,b}$ or $\nu_{17a,b}$) are significantly less effective than the a_{2u} mechanism, which, unlike the e_{2u} modes, preserves the nodal pattern of the E_{1g} and E_{1u} states.

B. Pyridine

1. Hyper-Rayleigh scattering

The HRlS spectrum of pyridine is shown in Fig. 4. HRlS in pyridine, unlike benzene, is allowed in the dipole approximation. The measured HRlS signal is about 50 times more intense than the strongest HRS band in pyridine. The bandwidth (FWHM) is 16 cm^{-1}. Separation of the contribution of cooperative HRlS from the measured line shape would require polarization-dependent measurements of the scattering.[2] We assume, however, that rotational diffusion dominates the observed linewidth.[5]

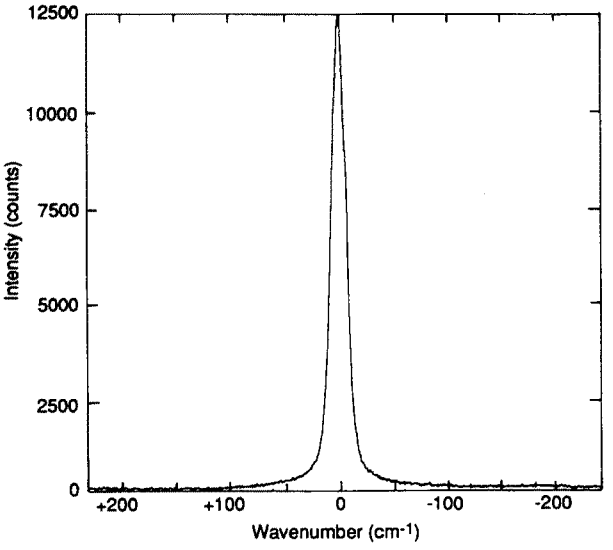

FIG. 4. Hyper-Rayleigh spectrum of pyridine excited at 1064 nm. Peak signal is 12 500 counts per channel collected in a total of nine Reticon exposures of 132 s per exposure.

2. Hyper-Raman scattering

Figure 5 presents the HRS spectum of pyridine excited at 1064 nm, together with the Raman spectrum excited at 532 nm. (See also Table I.) The dominant bands in the HRS spectrum are 704 cm^{-1} (b_1), 747 cm^{-1} (b_1), 1067 cm^{-1} (a_1,b_2) and 1225 cm^{-1} (a_1,b_2). (Labels of irreducible representations are with respect to an axis system where the molecule is in the yz plane and z is the axis of symmetry.) The 704 cm^{-1} fundamental ν_{11} correlates with the a_{2u} vibration of benzene at 671 cm^{-1} which was observed in our HRS spectrum of benzene. Fundamentals at 1144 cm^{-1} (b_2) and 994 cm^{-1} (a_1) are weak but discernible in the spectrum.

Vibrations in pyridine possess a much richer source of HRS intensities than the corresponding benzene vibrations. This is so firstly because the nonbonding electrons of pyridine lead to a more complex manifold of excited states ($n\pi^*$ and Rydberg states). Secondly, the lower symmetry permits vibronic coupling pathways that are forbidden in benzene. Thirdly, the Condon-allowed A term can conribute in preresonance and resonance HRS. At this point we can only discuss vibronic coupling pathways intuitively and speculatively. Calculations of vibronic-coupling matrix elements would clearly be helpful.

Not surprisingly, the vibration ν_{11} (b_1) at 704 cm^{-1}, corresponding to the a_{2u} mode observed in benzene, is also one of the strongest bands in the HRS spectrum of pyridine. It can derive intensity as it apparently does in benzene, by vibronic coupling of a two-photon allowed 3s Rydberg state (A_2) at 200 nm[37] formed by promotion of an electron from

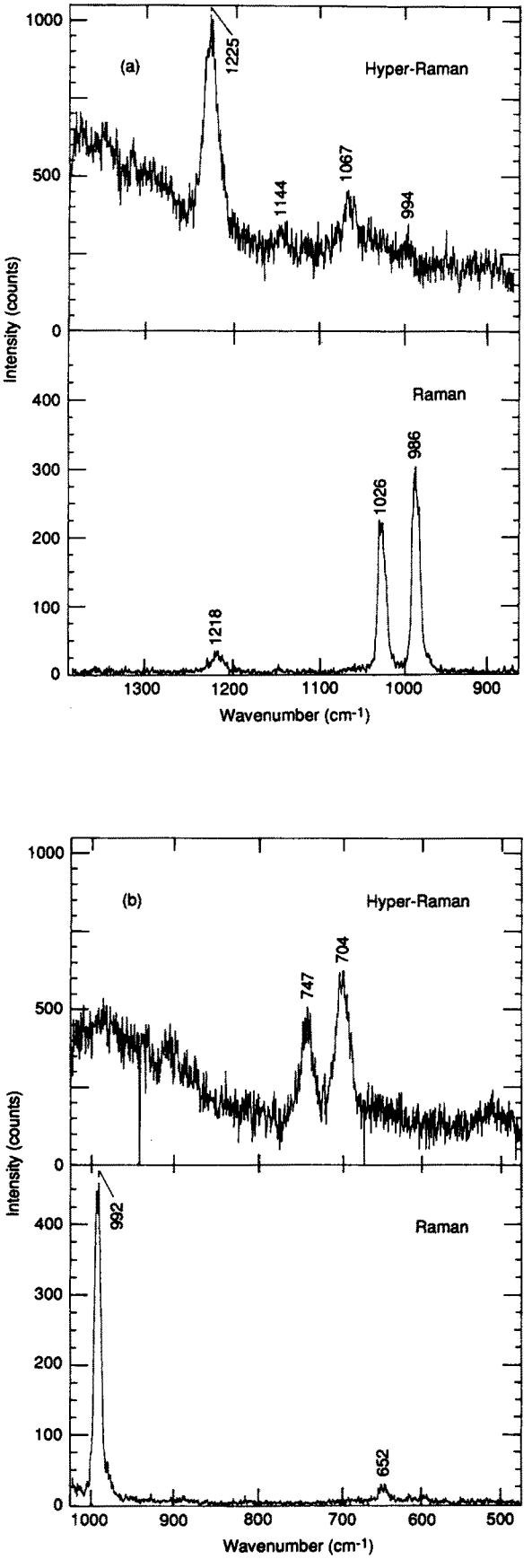

FIG. 5. Hyper-Raman and Raman spectra of pyridine; (a) 900–1350 cm^{-1} region. (b) 500–1000 cm^{-1} region. The HRS spectra are the sum of 25 Reticon exposures of 132 s per exposure. The Raman spectra were recorded in one exposure of 0.63 s. The HRS spectra were excited at 1064 nm, and the Raman spectra were excited at 532 nm.

TABLE I. Hyper-Raman bands in pyridine.

Wave number (cm^{-1})	Assignment		Experimental intensity[a]	Calculated intensity[b]
403	ν_{16b}	(b_1)	19?[c]	···
602	ν_{6a}	(a_1)	···	14
650	ν_{6b}	(b_2)	···	13
704	ν_{11}	(b_1)	88	···
747	ν_4	(b_1)	56	···
994	ν_1	(a_1)	11	13
1032	ν_{12}	(a_1)	···	54
1067	ν_{18b},ν_{18a}	(b_2,a_1)	21	97,15
1144	ν_{15}	(b_2)	8	20
1225	ν_3,ν_{9a}	(b_2,a_1)	100	100,17
1375	ν_{14}	(b_2)	···	16
1439	ν_{19b}	(b_2)	···	46
1572	ν_{8b}	(b_2)	···	20
1583	ν_{8a}	(a_1)	···	56

[a] Relative intensities. 100 corresponds to 610 counts at peak in sum of 25 Reticon scans for 3300s total collection time.
[b] Reference 19.
[c] Not shown. The reliability of this observation of this mode is still in question.

the highest occupied π molecular orbital, with the strongly allowed B_2 $\pi\pi^*$ state at 180 nm[37,38] (corresponding to the benzene E_{1u} state). The A_2 $n\pi^*$ state (245 nm) probably does not play an important role, since its participation in two-photon absorption is weak.[39] Other vibronic coupling pathways are also possible. For example, the A_1 $\pi\pi^*$ state around 207 nm, strongly allowed in two-photon absorption,[39] could couple vibronically with a B_1 one-photon allowed state. The other intense b_1 mode observed is ν_4 (747 cm^{-1}). This mode moves adjacent ring atoms out of the plane in opposite directions. Thus, it is expected to couple together states with different nodal patterns. For example, it may induce A_1 ($\pi\pi^*$) character (three nodal planes) into the B_1 Rydberg ($3p$) state.

The strongest band in the spectrum is that at 1225 cm^{-1}. This could be either the ν_3 (b_2) or the ν_{9a} (a_1) mode, or both. Since in the calculated *bulk* HRS spectrum[19] ν_3 is predicted to be the strongest band, we prefer to assign this band to ν_3, although this assignment cannot be made with any certainty. A likely source of intensity in ν_3 is vibronic coupling between the nearly degenerate strongly allowed A_1 and B_2 $\pi\pi^*$ states at 180 nm (corresponding to the degenerate strongly allowed benzene E_{1u} states). The torsional motion of this mode, with all six atoms of the ring moving together, is expected to couple these modes efficiently. Similarly, the band observed at 1067 cm^{-1} is either ν_{18a} (a_1) or ν_{18b} (b_2) or both. Of these two, the b_2 mode (ν_{18b}) was calculated to possess the greater bulk hyper-Raman intensity.[19] This is a torsional mode which could acquire intensity by a mechanism similar to the one described for ν_3. The only other b_2 vibration detected, ν_{15} (1144 cm^{-1}), is also a torsional mode.

Aside from possible contributions of ν_{9a} (1225 cm^{-1}) and ν_{18a} (1067 cm^{-1}), the only totally symmetric vibration observed is the weak band at 994 cm^{-1} (ν_1). Numerous vibronic coupling pathways are available for totally symmetric vibrations. Three A_1 states (two $\pi\pi^*$ states and a Ryd-

berg state) are thought to lie in close proximity between 207 and 182 nm.[37] These modes can also derive intensity by preresonance enhancement of the A term, as described by Eq. (16), and may become more prominent with excitation at shorter wavelength.

Golab *et al.*[19] have reported a calculation of both the bulk and surface-enhanced HRS spectra of pyridine. Their method employed a Pariser–Parr–Pople (PPP) calculation of the derivatives of the hyperpolarizability with respect to normal-mode coordinates. Relative intensities in their calculated HRS spectrum of bulk pyridine are included in Table I. A comparison can now be made between their calculated bulk HRS spectrum and the experimentally observed spectrum. The most intense band in the calculated spectrum, the 1230 cm^{-1} b_2 vibration (ν_3), is also the most intense in our HRS spectrum. However, mode ν_{18b} (b_2), which was calculated to be nearly as intense as ν_3, is weaker in the observed spectrum. Modes ν_{12}, ν_{19b}, and ν_{8a} were also calculated to have significant intensity, but were not detected in our HRS spectrum. Thus, while theory and experiment agree qualitatively on some of the in-plane modes, there are significant differences in relative intensity. The out-of-plane bands observed at 704 and 747 cm^{-1} in Fig. 5 cannot be treated by PPP theory.[19]

It is interesting to compare the relative intensities (see Table I) in the HRS spectrum in Fig. 5 to those in the reported surface-enhanced hyper-Raman spectrum (SEHRS) for pyridine on silver,[19] also generated by 1064 nm excitation. The most intense bands in the surface spectrum are the totally symmetric modes ν_{8a}, ν_1, and ν_{12}, and a band at 1214 cm^{-1}, assigned to the totally symmetric vibration ν_{9a}. These are also the strongest bands in the SERS spectrum of pyridine on silver. In contrast, the most intense modes in the HRS spectrum of bulk pyridine are the out-of-plane vibrations ν_4 and ν_{11}, and the 1225 cm^{-1} band $\nu_3(b_2)$ or $\nu_{9a}(a_1)$. Furthermore, while mode ν_{6a} (625 cm^{-1}) is moderately intense in the reported SEHRS and SERS spectra, it was too weak to observe in our HRS spectrum. Thus in general, the SEHRS spectrum reported by Golab *et al.* bears a greater resemblence to the SERS spectrum than to the bulk HRS spectrum. The reasons for the difference between the bulk HRS and the SEHRS spectra and the similarity between the SEHRS and SERS spectra need further investigation, but may be related to the enhanced electric field perpendicular to the surface and parallel to the z axis of the molecule (assuming a perpendicular orientation of pyridine on the surface). This would lead to an enhancement of the β_{zzz} component of the hyperpolarizability, which has a_1 symmetry.[24] Selective surface enhancement of totally symmetric modes in both SERS and SEHRS was predicted by the PPP calculation with the assumption of a perpendicular orientation of the molecule on the surface.

V. SUMMARY

We have reported the first HRS spectra of benzene and pyridine. The strongest bands observed in these spectra are (1) out-of-plane vibrational modes and (2) in pyridine, modes involving torsional motion of the ring atoms. The theory of vibronic coupling in HRS shows that, as in nonresonant Raman scattering, nonresonant HRS is vibronically induced. In noncentrosymmetric molecules, the Condon term can contribute to preresonance and resonance HRS. The observation of the prominent bands in the HRS spectra of benzene and pyridine can be explained qualitatively by likely vibronic coupling pathways in these molecules. These pathways differ from those observed in one- and two-photon spectroscopies, and involve vibrations that couple one- and two-photon allowed states effectively. Calculations are clearly needed to understand vibronic coupling in HRS in a more qualitative way. Experiments with preresonant and resonant two-photon excitation would help to elucidate the participation of various excited states in HRS. The HRS spectrum in pyridine was compared to a calculated HRS spectrum for bulk pyridine, and to the reported surface-enhanced spectrum.[19] The spectral intensities predicted by PPP theory are at best qualitatively correct.

Hyper-Rayleigh scattering was also observed in benzene and pyridine. The HRlS in pyridine is strong, as expected for a noncentrosymmetric species. In benzene, weak HRlS was observed, and attributed to collective motions in the liquid. The much larger linewidth in benzene HRlS than in pyridine HRlS reflects the fast relaxation of the operative intermolecular correlation functions.

HRS, while still experimentally challenging, offers the spectroscopist a unique tool for probing molecular vibrations and molecular excited states. In centrosymmetric molecules, it is a probe particularly sensitive to vibronic coupling and exposes vibronic coupling mechanisms not accessed by other spectroscopic methods. HRlS, on the other hand, offers a potentially rich source of information on liquid-state dynamics, especially for collective motions. While the contribution of collective motions to HRlS can be extracted from the HRlS profile for noncentrosymmetric molecules only with some difficulty, it is the dominant contributor to HRlS in centrosymmetric molecules

ACKNOWLEDGMENT

Acknowledgment is made to the donors of The Petroleum Research Fund, administered by the ACS, for support of this research.

[1] R. Bersohn, Y. H. Pao, and H. L. Frisch, J. Chem. Phys. **45**, 3184 (1966).
[2] P. D. Maker, Phys. Rev. A **1**, 923 (1970).
[3] S. Kielich, Bull. Acad. Polon. Sci. **12**, 53 (1964); S. Kielich, J. R. Lalanne, and F. B. Martin, Phys. Rev. Lett. **26**, 1295 (1971).
[4] W. Alexiewicz, T. Bancewicz, S. Kielich, and Z. Ozgo, J. Raman Spectrosc. **2**, 529 (1974).
[5] V. N. Denisov, B. N. Marvin, and V. B. Podobedov, Phys. Rep. **151**, 1 (1987).
[6] R. W. Terhune, P. D. Maker, and C. M. Savage, Phys. Rev. Lett. **14**, 681 (1965).
[7] M. J. French and D. A. Long, J. Raman Spectrosc. **3**, 391 (1975).
[8] W. J. Schmid and H. W. Schroetter, Chem. Phys. Lett. **45**, 502 (1977).
[9] A. Hiraya, Y. Udagawa, and M. Ito, Chem. Lett. **4**, 433 (1979).
[10] T. J. Dines, M. J. French, R. J. B. Hall, and D. A. Long, J. Raman Spectrosc. **14**, 225 (1983).
[11] V. N. Denisov, B. N. Mavrin, V. B. Podobedov, and K. E. Sterin, J. Raman Spectrosc. **16**, 71 (1985).
[12] Y. Murioka and I. Nakagawa, Chem. Phys. Lett. **122**, 150 (1985); A. M. Agal'tov, V. S. Gorelik, and M. M. Sushchinskii, Opt. Spektrosk. **58**, 386 (1985).

[13]H. Vogt and H. Presting, Phys. Rev. B **31**, 6731 (1985); V. N. Densiov, B. N. Mavrin, V. B. Podobedov, K. E. Sterin, and B. G. Varshal, J. Non-Cryst. Solids **64**, 195 (1984).
[14]J. S. Horowitz, B. E. Kohler, and T. A. Spiglanin, J. Phys. Chem. **89**, 1574 (1985).
[15]L. D. Ziegler and J. L. Roebber, Chem. Phys. Lett. **136**, 377 (1987); L. D. Ziegler, Y. C. Chung, and Y. P. Zhang, J. Chem. Phys. **87**, 4498 (1987).
[16]Y. C. Chung and L. D. Ziegler, J. Chem. Phys. **88**, 7287 (1988).
[17]A. V. Baranov, Y. S. Bobovich, and N. P. Vasilenko, Opt. Spectrosc. (USSR) **61**, 490 (1986), and references therein.
[18]D. V. Murphy, K. U. Von Raben, R. K. Chang, and P. B. Dorian, Chem. Phys. Lett. **85**, 43 (1982).
[19]J. T. Golab, J. R. Sprague, K. T. Carron, G. C. Schatz, and R. P. Van Duyne, J. Chem. Phys. **88**, 7942 (1988).
[20]Stimulated Raman scattering is unlikely to generate a significant population of excited vibrational levels in our experiment due to the short beam waist length (Rayleigh range) over which this intensity is reached with the short focal length employed. For the 992 cm^{-1} mode of benzene we estimate the stimulated gain coefficient $G_R \lesssim 1$. See Y. R. Shen, *The Principles of Nonlinear Optics* (Wiley-Interscience, New York, 1984), p. 145.
[21]D. A. Long and L. Stanton, Proc. R. Soc. London Ser. A **318**, 441 (1970).
[22]D. L. Andrews and T. Thirunamachandran, J. Chem. Phys. **68**, 2941 (1978).
[23]S. J. Cyvin, J. E. Rauch, and J. C. Decius, J. Chem. Phys. **43**, 4083 (1965).
[24]J. H. Christie and D. J. Lockwood, J. Chem. Phys. **54**, 1141 (1971).
[25]L. Stanton, J. Raman Spectrosc. **1**, 53 (1973).
[26]V. I. Petrov, Opt. Spectrosc. (USSR) **59**, 284 (1986).
[27]J. Tang and A. C. Albrecht, in *Raman Spectroscopy*, edited by H. A. Szymanski (Plenum, New York, 1970), Vol. 2 p. 33.
[28]G. J. Small, J. Chem. Phys. **62**, 4661 (1975).
[29]E. S. Yeung, M. Heiling, and G. J. Small, Spectrochim. Acta Part A **31**, 1921 (1975).
[30]S. Kielich, Prog. Opt. **20**, 155 (1983).
[31]S. Kielich, J. R. Lalanne, and F. B. Martin, J. Raman Spectrosc. **1**, 119 (1973); Acta Phys. Pol A **41**, 479 (1972).
[32]V. N. Denisov, B. N. Mavrin, and V. B. Podobedov, Opt. Spectrosc. USSR **57**, 584 (1984).
[33]T. W. Scott and A. C. Albrecht, J. Chem. Phys. **74**, 3807 (1981).
[34]E. B. Wilson, J. C. Decius, and P. C. Cross, *Molecular Vibrations* (Dover, New York, 1980), p. 260.
[35]D. P. Gerrity, L. D. Ziegler, P. B. Kelly, R. A. Desiderio, and B. Hudson, J. Chem. Phys. **83**, 3209 (1985).
[36]R. L. Whetten, K. J. Fu, and E. R. Grant, J. Chem. Phys. **79**, 2626 (1983).
[37]A. Bolovinos, P. Tsekeris, J. Philis, E. Pantos, and G. Andritsopoulos, J. Mol. Spectrosc. **103**, 240 (1984).
[38]K. K. Innes, J. P. Byrne, and I. G. Ross, J. Mol. Spectrosc. **22**, 125 (1967).
[39]P. R. Salvi, P. Foggi, R. Bini, and E. Castellucci, Chem. Phys. Lett. **141**, 417 (1987).